Geosphere, published online on 6 March 2013 as doi:10.1130/GES00812.1
The ANDRILL McMurdo Ice Shelf (MIS) and Southern McMurdo Sound (SMS) Drilling Projects themed issue

Alteration of volcanic deposits in the ANDRILL AND-1B core: Influence of paleodeposition, eruptive style, and magmatic composition

Alessio Di Roberto[1], Giovanna Giorgetti[2], Francesco Iacoviello[2], and Massimo Pompilio[1]
[1]*Istituto Nazionale di Geofisica e Vulcanologia, sezione di Pisa, Via della Faggiola, 32-56126 Pisa, Italy*
[2]*Dipartimento di Scienze della Terra–Università degli Studi di Siena, Via Laterina, 8-53100 Siena, Italy*

ABSTRACT

Alteration minerals, assemblages, and textures were studied in a 175-m-thick volcanic sequence found between 759.32 and 584.19 m below seafloor within the 1285-m-long ANDRILL (Antarctic Geological Drilling project) McMurdo Ice Shelf core (MIS AND-1B). Three main alteration zones were identified through the application of different analytical methods (optical and scanning electron microscopy, electron microprobe, and X-ray diffraction). Alteration zoning is guided by the texture of the volcanic deposits, which is in turn determined by the eruptive style, transport mechanisms, and paleodepositional conditions. In particular, alteration reflects the evolution of paleodepositional conditions from submarine or shallow water to subaerial due to the growth of a nearby volcanic edifice. The general alteration trend is also influenced by the contribution of volcanogenic sediments derived from the reworking of silica-rich pyroclasts from earlier volcanic activity.

INTRODUCTION

The ANDRILL (Antarctic Geological Drilling project) AND-1B core contains a well-preserved (>98% core recovery), high-resolution late Neogene record of the nearshore glacimarine environment in Antarctica (Naish et al., 2007, 2009). The marine core was drilled at a water depth of 943 m beneath the McMurdo Ice Shelf, in the Ross Embayment of Antarctica (Fig. 1). The McMurdo Ice Shelf drill site is located ~10 km east of Hut Point Peninsula, in the subsidence moat created by the volcanic Ross Island (Naish et al., 2007).

Recovered sediments have been interpreted in terms of changing environmental conditions since ca. 12 Ma (McKay et al., 2009; Naish et al., 2009). The 1285-m core consists of intercalated glacigenic, biogenic, and volcanic deposits. Volcanic rocks form a significant component of the core and compose ~70% of the total clast count (Pompilio et al., 2007); they are found both in glacigenic sediments and in thick, discrete volcanic layers.

An ~175-m-thick and continuous volcanic succession is between 584.19 and 759.32 m below the seafloor (mbsf). This volcanic lithostratigraphic unit (LSU5) is also characterized by the absence of diatomite and by a wide range of siliciclastic sediments (Krissek et al., 2007; Di Roberto et al., 2010). LSU5 includes different lithologies that were interpreted to record the evolution of a volcanic complex from submarine to shallow water and/or emergent conditions with related glacio-volcanic gravity flow processes (Krissek et al., 2007; Di Roberto et al., 2010). These volcanic rocks show different degrees of alteration that increase with depth (Di Roberto et al., 2010).

Numerous studies (Schiffman et al., 2000; Walton and Schiffman, 2003, and references therein) and reviews (e.g., Honnorez, 1981; Fisher and Schmincke, 1984; Singer and Banin, 1990; Stroncik and Schmincke, 2002) have explored in detail the alteration of volcanic rocks during low-temperature interaction with aqueous fluids, focusing on the formation of alteration phases (mainly palagonite) and on the compositional changes attending the alteration processes. Because of its thermodynamic instability, volcanic glass is highly reactive and is therefore able to record relevant changes in physical and chemical conditions during syneruptive and posteruptive processes. Alteration textures and mineral assemblages that derive from glass modification can give information on the environment of deposition and successive modification due to deposit burial and diagenesis. For example, the study of low-temperature alteration of glass-bearing volcanic deposits can provide information on glass-fluid interaction and temperature, duration of interaction, fluid properties, and nature of the primary material (Stroncik and Schmincke, 2002, and references therein). On this basis, we focus here on the analysis of different alteration minerals, assemblages, and textures in the LSU5 unit to understand the postdepositional processes that affected the glass-bearing volcanic deposits. We thus also relate postdepositional processes to paleodepositional conditions and style of eruptive activity.

LSU5 STRATIGRAPHY AND DEPOSITIONAL ENVIRONMENTS

LSU5 includes a number of different lithologies, i.e., hyaloclastites, tuffs and lapilli tuffs, volcaniclastic diamictites, a submarine lava flow, and volcanic glass shard–rich sandstones to mudstones representing different eruptive and volcano-sedimentary processes as well as alteration environments (Krissek et al., 2007; Di Roberto et al., 2010). A brief description of the different lithologies is given in the following (for more details, see Di Roberto et al., 2010).

Lapilli Tuff and Tuff

The lapilli tuff and tuff lithologies comprise centimeter to decimeter thick beds of massive to crudely stratified hyaloclastite, tuff, and lapilli tuff consisting of juvenile glassy fragments (pumice, scoria, and glass shards) mixed with minor amounts of loose crystals of feldspar and minor clinopyroxene, poorly vesicular lava fragments, and lithics (reddish oxidized lava clasts). Hyaloclastite, tuff, and lapilli tuff are commonly grain supported and generally characterized by an open frame texture. Secondary pores between grains are occupied by calcite, zeolite, and minor clay minerals. The vitric fragments preserve fragile structures (i.e., glass vesicle walls) and have not been significantly reworked.

Geosphere; April 2013; v. 9; no. 2; doi:10.1130/GES00812.1; 7 figures; 3 tables.
Received 16 April 2012 ♦ Revision received 20 November 2012 ♦ Accepted 20 December 2012 ♦ Published online 6 March 2013

For permission to copy, contact editing@geosociety.org
© 2013 Geological Society of America

Geosphere, published online on 6 March 2013 as doi:10.1130/GES00812.1

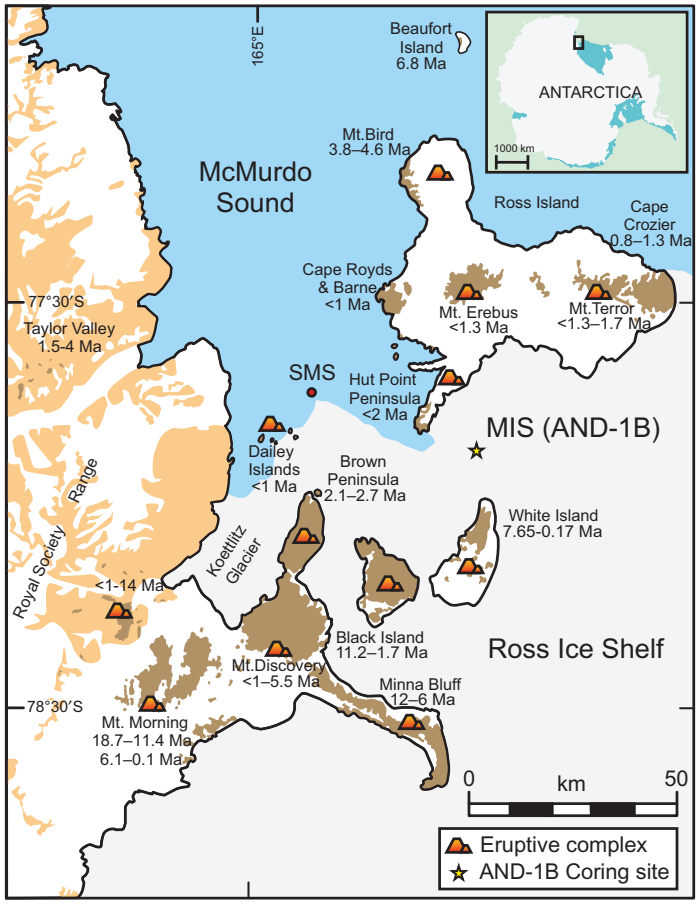

Figure 1. Map of southern Victoria Land, Antarctica, showing the location of the ANDRILL (Antarctic Geological Drilling project) AND-2A Southern McMurdo Sound (SMS) core site and relevant geological features of the Erebus Volcanic Province (redrawn from Del Carlo et al., 2009). The map also shows outcrops of volcanic rocks belonging to the McMurdo Volcanic Group and the relative timing of activity according to K-Ar and ^{40}Ar-^{39}Ar ages (Mercer, 1968; Kyle and Cole, 1974; Mayewski, 1975; Armstrong, 1978; Kyle, 1981, 1990a, 1990b; Kyle and Muncy, 1989; Wright and Kyle, 1990a, 1990b; McKelvey et al., 1991; Wilch et al., 1993; Marchant et al., 1996; Esser et al., 2004; Tauxe et al. 2004; Timms, 2006; Cooper et al., 2007; Lewis et al., 2007; Wilch et al., 2008; Martin et al., 2010). MIS (AND-1B)—McMurdo Ice Shelf core.

Volcanic Diamictite

Volcanic diamictites consist of gray to black, dense to poorly vesicular clasts produced by rapid quenching and fragmentation of submarine lavas (autoclastic) admixed with volcanic clasts texturally similar to those forming tuff and lapilli tuff (pyroclastic). Lava fragments are characterized by a fine-grained pilotaxitic groundmass with a few <2 mm phenocrysts of feldspar and minor clinopyroxene (Di Roberto et al., 2010). The diameters of clasts range from a few hundred microns to several centimeters. Volcanic diamictites vary from clast to matrix supported. The matrix consists of silt-sized material frequently altered to clay minerals. As in tuff, vitric fragments show fragile structures (i.e., glass vesicle walls) and have not been significantly reworked.

Lava Flow

The lava flow is a fine-grained tephrite bearing a few large (>1 mm) feldspar phenocrysts set in a pilotaxitic groundmass with <250 µm microcrystals of feldspar and clinopyroxene.

Volcanic Clast–Rich Mudstones to Sandstones

Volcanic clast–rich mudstones to sandstones consist of turbiditic sandstones to siltstones, interlaminated and interbedded (Krissek et al., 2007; Di Roberto et al., 2010). Sediments are a mixture of sand- to silt-sized volcanic and nonvolcanic clasts with abundant fragments of lava, scoria, pumice, and magmatic crystals (feldspar and clinopyroxene) admixed with granitoids, metasediments, and mudstone clasts. Vitric fragments embedded in the volcanic-rich mudstone and sandstone are often abraded and rounded, thus testifying to major reworking.

The LSU5 sequence was divided into two main subunits, LSU5A and LSU5B, on the basis of the nature, texture, and composition of sediments (Di Roberto et al., 2010).

The LSU5A extends between 688.92 and 759.32 mbsf and mainly consists of a monothematic sequence of stacked volcanic-rich mudstones to sandstones (volcanogenic mudstone to sandstone) deposited by turbidity currents and gravity flow processes. In Di Roberto et al. (2010), it was suggested that the turbidity currents were generated from a distal grounding line and supplied fine sediment produced by fluvial and glacial erosion of volcanic and basement rocks; it was also suggested, alternatively, that the LSU5A sediments may have originated from the mixing of fine-grained primary volcaniclastic deposits with nonvolcanic detritus supplied by glacier tongues descending from the Transantarctic Mountain front and by grounding-line processes. This second environmental interpretation seems to be supported by the presence of pyroclastic deposits, namely primary tuff and lapilli tuff beds (likely deposited by eruption-fed turbidity currents; White, 2000) and resedimented syneruptive volcanogenic deposits (volcanic diamictites) in the upper portion of LSU5A (~15 m). These indicate that the system was increasingly dominated by materials directly derived from subaqueous volcanic activity close to the drill site (Di Roberto et al., 2010).

The ~105-m-thick upper LSU5B subsequence and the lower few meters of LSU4.4 extending between 584.19 and 688.92 mbsf consist mainly of interbedded pyroclastic deposits (hyaloclastite, tuff, and lapilli tuff) and resedimented syneruptive volcanogenic deposits (volcanic diamictite) and a ~3-m-thick subaqueous lava flow dated as Late Miocene (6.48 Ma; Wilson et al., 2012). Pyroclastic deposits and resedimented syneruptive volcanogenic deposits are punctuated by intervals of volcanogenic sedimentary deposits (volcanic-rich sandstones to siltstones) as much as several meters thick that

Geosphere, published online on 6 March 2013 as doi:10.1130/GES00812.1

are laminated to massive and frequently bioturbated. LSU5B was attributed to repeated cycles of submarine to emergent explosive to effusive volcanic activity, with occasional periods of quiescence lasting as long as 1 m.y. (Di Roberto et al., 2010).

METHODS

A total of 60 samples were collected between 575.65 and 759.32 mbsf for observation and analysis (Table 1). All samples were observed and described using an optical microscope. Polished thin sections from 11 samples representative of the main lithologies (Table 2) were examined using a scanning electron microscope at the Dipartimento di Scienze della Terra (Università di Siena, Italy). A Philips XL30 instrument operated at 20 kV and equipped with an EDAX DX4 energy-dispersive system (EDS) was used to complete the chemical analysis of smectites. X-ray diffraction (XRD) analyses were performed on 30 selected samples in order to characterize the mineralogy of the clay fraction; the average sample spacing was ~6 m. The clay fraction was separated and analyzed following standard procedures (Ehrmann et al., 1992; Petschick et al., 1996). XRD measurements were conducted with an automated Philips PW1710 powder diffraction system using CuKα radiation (40 kV, 40 mA). Each sample was analyzed between 2° and 40° 2θ, with a step size of 0.02° 2θ, in the air-dry state and after ethylene glycol solvation. A slow scan between 23° and 25.5° 2θ with a step size of 0.005° 2θ was performed on the glycolated samples to obtain a better resolution of the chlorite-kaolinite twin peaks. Diffractograms were processed using the MacDiff software (Petschick, 2001; Frankfurt University, Germany) to determine the abundance of the main clay minerals (smectite, illite, chlorite, and kaolinite) using the weighting factors of Biscaye (1965). Clay mineral percentage standard deviations were calculated using the results of 10 diffractograms obtained from 10 oriented mounts prepared from a single sample. Standard deviations were illite ±1%, smectite ±1%, chlorite ±2.5%, and kaolinite ±2%. Major element glass composition and mineral analyses were performed at the HPHT (high pressure, high temperature) Laboratory of Istituto Nazionale di Geofisica e Vulcanologia (Sezione di Roma, Italy) using a JEOL JXA 8200 microprobe equipped with 5 wavelength-dispersive spectrometers and an EDS analytical system. Between 20 and 30 spot analyses were performed on each sampled volcanic fragment and on each specimen of the sediment matrix or cement. Operating conditions were 15 kV accelerating voltage, 5 nA beam current, 5 µm probe diameter, and 10 s and 5 s acquisition time for peak and background, respectively.

Nomenclature used herein to classify volcaniclastic rocks and to describe alteration degree refers to Houghton and Wilson (1989) and McPhie et al. (1993), and Gifkins et al. (2005), respectively.

RESULTS

Alteration Texture and Phases

Sediments at depths shallower than 584.61 mbsf are mostly constituted of light brown sideromelane, tachylite, and vitric lava clasts that are not altered (Fig. 2A). Calcite and rare phillipsite occur as intergranular cement.

Between 584.61 and 591.85 mbsf sediments are formed by vitric clasts with subtle alteration (Fig. 2B). The sideromelane and tachylite fragments are frequently fractured and, in some cases, a layer of hydrated glass tens of microns thick surrounds the external surface of the grains (Figs. 3A, 3B). In addition, patchy transformation of glass into palagonite and palagonite vesicle linings occur together with minor smectite pore linings (Figs. 3A–3C). Phillipsite (Fig. 2B) also occurs as white to pale pink (plane-polarized transmitted light) fibroradial to spherulitic masses filling volcanic vesicles and secondary pores (fractures and dissolution pits) and mostly constitutes the sediment cement. Minor analcime occurs as late infilling of primary and secondary pores (Fig. 2B). Calcite occasionally fills porosity created by glass dissolution, vesicles, and pores (Figs. 2D and 3C) or forms a part of intergranular matrix. Above 591.85 mbsf volcanic textures of vitric fragments, including external shape and original vesicularity, are mostly preserved.

Sediments at depth >591.85 mbsf are weakly to moderately altered. No fresh glass is preserved. The alteration mineral assemblage consists of phillipsite, analcime, calcite, and apatite in both primary and secondary pores, and TiO_2 micronodules (Figs. 2C–2F, 3D, and 3E). Within hyaloclastite, tuffs, and volcanic diamictites, alteration of vitric fragments commonly includes grain fracturing, glass dissolution along external grain surfaces, smectite grain coating, smectite and palagonite vesicle lining, complete conversion of volcanic glass into palagonite, and replacement of volcanic glass by analcime (Figs. 2C–2F and 3D–3F) or clay minerals. In contrast, volcanic clast–rich sandstones and siltstones are constituted of variably altered clasts embedded in a fine matrix of clay minerals. Vitric clasts are often substituted by analcime and calcite (Fig. 3F). Primary and secondary pores are filled by analcime, palagonite, and smectites, whereas palagonite may form a fine outer rim. In all types of sediment at depths >591.85 mbsf, calcite fills porosity created by glass dissolution, vesicles, and pores (Fig. 3D) or coexists with analcime and smectite in the intergranular matrix. Pyrite crystals a few tens of microns in size and pyrite aggregates were identified on the outer edge of the lava flow, around the quenched, glassy outer surface of lava fragments and in vesicle fillings. In the very first meters below the depth of 591.85 mbsf most of the original volcanic textures are preserved; downcore most of the fragile volcanic textures such as thin vesicle septa in pumice, fibrous structures in fluidal clasts, and volcanic vesicles are modified or destroyed by the alteration process.

Mineralogical and Chemical Composition

Glasses that occur in samples shallower than 591.85 mbsf have homogeneous basanitic composition (Table 2; Fig. 4) and are unaltered (total oxides >97 wt%).

Between 584.61 and 591.85 mbsf, sideromelane is slightly altered and transformed into palagonite (Table 2). Palagonitized glass has low total oxides (<95 wt%) and is generally depleted in all major elements (Table 2; Fig. 4) with respect to average unaltered glass (Fig. 4), whereas it is enriched in TiO_2, MgO, and total iron (FeO remains unchanged).

At depths >591.85 mbsf, the volcanic glass underwent major alteration involving significant chemical and physical changes (Table 2; Fig. 4). The composition of palagonite formed from basanitic glass within hyaloclastite, tuff, and volcanic diamictites is almost constant, with only minor variation (Table 2; Fig. 4). Compositions plotted in Mg/(Mg + Fe) and Al/(Al + Si) versus Na + K + Ca diagrams (cations were calculated on the basis of 22 oxygen equivalents) show that the chemical changes involved in the palagonitization of fresh basanitic glass are a depletion in Na + K + Ca, a decrease in the Al/(Al + Si) ratio, and an increase in the Mg/(Mg + Fe) ratio (circles and diamonds in Fig. 5). Volcanic glass found within volcanic-rich sandstones at 611.35, 716.23, and 747.09 mbsf is generally less altered compared to altered sideromelane in hyaloclastite, tuff, and volcanic diamictites. The glasses found within volcanic-rich sandstones have relatively high total oxides (~90 wt%), are more silica rich, and have an almost constant trachytic to rhyolitic composition (Table 2; Fig. 4). In the Mg/(Mg + Fe) and Al/(Al + Si) versus Na + K + Ca diagrams (squares in Fig. 5), the composition of glass found within volcanic-rich sandstones display fairly constant Na + K + Ca values

TABLE 1. SAMPLES EXAMINED DURING THIS STUDY, PERFORMED ANALYSES AND MAIN OBSERVED ALTERATION TEXTURE AND MINERAL

			Analyses			Alteration phases and textures								
Sample, depth	LSU	Lithology	SEM	EMP	XRD	Fresh glass	Palagonite	Smectite	Zeolite	Calcite	Pyrite	TiO_2-rich nodules	Grain fracturing	Grain dissolution
AND 1B 575.65	4.4	Al	•		•	•								
AND 1B 575.68	4.4	Al				•								
AND 1B 578.85	4.4	VRS				•				•				
AND 1B 579.25	4.4	VRS		•		•				•				
AND 1B 579.85	4.4	VRS				•				•				
AND 1B 584.61	4.4	Hyalo		•	•	•								
AND 1B 588.63	5B	LT	•			•	•	•	P/A	•		•	•	
AND 1B 591.85	5B	LT	•	•	•	•	•	•	P/A	•		•		
AND 1B 595.05	5B	VD					•	•	A	•			•	•
AND 1B 595.79	5B	T			•		•	•	A			•		•
AND 1B 599.86	5B	VRS					•	•	A					•
AND 1B 600.05	5B	T		•	•		•	•	A	•		•		•
AND 1B 602.80	5B	LT	•	•			•	•	A	•		•	•	•
AND 1B 602.85	5B	LT	•	•			•	•	A		•	•	•	•
AND 1B 603.06	5B	T			•		•	•	A		•	•		•
AND 1B 603.74	5B	LT					•	•	A	•				•
AND 1B 605.39	5B	T			•		•	•	A	•				
AND 1B 608.73	5B	T			•		•	•	A					•
AND 1B 611.35	5B	VRS		•	•		•	•	A				•	•
AND 1B 615.44	5B	VRS			•		•	•	A			•		•
AND 1B 620.38	5B	VRS			•		•	•	A			•		•
AND 1B 620.80	5B	VD					•	•	A			•		•
AND 1B 622.22	5B	VD					•	•	A			•		•
AND 1B 622.83	5B	T	•				•	•	A					•
AND 1B 624.02	5B	VRS							A	•		•		•
AND 1B 636.40	5B	T	•		•		•	•	A			•		•
AND 1B 641.44	5B	VD	•				•	•	A			•		•
AND 1B 646.24	5B	VD	•		•		•	•	A			•		•
AND 1B 646.38	5B	LF	•					•	A		•			•
AND 1B 646.54	5B	LF					•	•	A		•	•		
AND 1B 652.81	5B	VD	•	•			•	•	A					•
AND 1B 656.66	5B	VD					•	•	A			•	•	•
AND 1B 657.56	5B	VD					•	•	A			•	•	•
AND 1B 658.03	5B	VD	•	•	•		•	•	A			•	•	•
AND 1B 662.65	5B	LT		•	•		•	•	A			•	•	•
AND 1B 663.91	5B	LT	•				•	•	A			•	•	•
AND 1B 668.01	5B	LT					•	•	A			•		•
AND 1B 678.38	5B	VD							A	•		•		•
AND 1B 678.9	5B	VD			•				A	•		•		•
AND 1B 679.68	5B	VD							A	•		•		•
AND 1B 680.36	5B	VD					•	•	A	•		•		•
AND 1B 681.75	5B	VD					•	•	A	•		•		•
AND 1B 683.38	5A	T			•		•	•	A			•		•
AND 1B 688.80	5A	T			•		•	•	A	•		•		•
AND 1B 692.74	5A	Hyalo			•		•	•	A			•		•
AND 1B 696.92	5A	Hyalo			•		•	•	A			•		•
AND 1B 702.19	5A	LT		•	•		•	•	A	•		•		•
AND 1B 711.02	5A	LT		•	•		•	•	A	•		•		•
AND 1B 716.23	5A	VRS		•	•				A			•		•
AND 1B 720.04	5A	VRS			•				A			•		•
AND 1B 720.22	5A	Hyalo							A					•
AND 1B 725.03	5A	VRS					•		A					•
AND 1B 730.64	5A	VRS					•	•	A	•		•		•
AND 1B 735.84	5A	VRS			•		•	•	A			•		•
AND 1B 745.12	5A	VRS			•				A	•		•		•
AND 1B 747.09	5A	VRS	•	•					A	•		•		•
AND 1B 748.97	5A	VRS	•						A	•		•		•
AND 1B 758.11	5A	VRS							A			•		•
AND 1B 758.25	5A	VRS			•				A			•		•
AND 1B 758.48	5A	VRS							A		•			

Note: AND—ANDRILL (Antarctic Drilling) McMurdo Ice Shelf core; depths in m below seafloor. LSU—lithostratigraphic unit; SEM—scanning electron microscopy; EMP—electron microprobe; XRD—X-ray diffraction; Al—Ash lens; Hyalo—Hyaloclastite; LF—Lava flow; LT—Lapilli Tuff; T—Tuff; VD—Volcanic Diamictite; VRS—Volcanic-rich Sandstone; P—Phillipsite; A—Analcime. From left to right, dots indicate: Analyses: what kind of analysis was performed on samples in the first column; Alteration phases: the presence of the mineral in each sample.

Geosphere, published online on 6 March 2013 as doi:10.1130/GES00812.1

TABLE 2. AVERAGE COMPOSITION OF GLASS AND PALAGONITE

	Unaltered glass		579.25 Al (bas)		584.61 Hyalo (bas)		591.85 LT (palag)	
Sample	avg. (n = 63)	Variance	avg. (n = 10)	Variance	avg. (n = 10)	Variance	avg. (n = 26)	Variance
SiO_2	43.88	0.94	43.65	1.37	43.30	0.16	38.26	27.59
TiO_2	3.75	0.15	3.29	0.34	4.25	0.00	4.39	2.94
Al_2O_3	15.71	0.74	15.74	0.34	15.79	0.01	11.23	10.72
FeO	11.06	0.44	10.42	0.94	10.69	0.37	11.90	17.35
MnO	0.22	0.00	0.24	0.00	0.26	0.01	0.21	0.01
MgO	4.39	0.73	3.77	0.32	4.40	0.17	8.80	23.56
CaO	10.28	1.69	9.55	1.96	10.23	0.18	5.45	4.66
Na_2O	4.74	0.39	4.00	0.88	1.94	0.21	0.98	1.71
K_2O	2.31	0.20	2.32	0.16	1.90	0.00	0.76	1.24
P_2O_5	1.31	0.17	1.11	0.01	1.99	0.00	1.06	0.52
Totals	97.65	0.30	94.08	4.19	94.76	1.13	83.03	121.97
	600.05 T (palag)		602.8 LT (palag)		611.35 VRS (trach)		652.81 VD (palag)	
Sample	avg. (n = 15)	Variance	avg. (n = 15)	Variance	avg. (n = 15)	Variance	avg. (n = 10)	Variance
SiO_2	30.32	46.78	29.75	27.60	63.85	7.56	35.80	7.28
TiO_2	7.08	15.63	5.71	12.11	0.44	0.00	0.48	0.03
Al_2O_3	5.79	12.11	5.65	2.74	14.20	5.73	6.35	0.45
FeO	11.77	26.72	12.25	14.33	1.17	0.02	19.41	4.87
MnO	0.22	0.02	0.19	0.01	0.07	0.00	0.35	0.00
MgO	6.17	4.55	8.23	7.09	0.46	0.00	10.29	0.46
CaO	8.01	7.20	9.30	9.88	3.52	1.59	1.96	0.27
Na_2O	2.06	5.43	0.78	0.02	4.10	12.32	2.21	0.04
K_2O	0.44	0.05	0.19	0.01	1.43	0.49	0.61	0.01
P_2O_5	1.04	1.66	1.44	0.84	0.16	0.01	0.04	0.00
Totals	72.91	68.30	73.49	126.95	89.40	0.00	77.50	40.18
	658.03 VD (palag)		662.65 LT (palag)		702.19 LT (palag)		711.02 LT (palag)	
Sample	avg. (n = 10)	Variance	avg. (n = 16)	Variance	avg. (n = 20)	Variance	avg. (n = 20)	Variance
SiO_2	27.96	20.80	24.94	7.18	23.04	11.71	25.53	16.49
TiO_2	6.31	13.83	8.90	5.84	9.84	47.83	8.99	5.99
Al_2O_3	5.91	2.31	4.37	0.34	4.20	4.45	4.50	0.55
FeO	15.59	21.53	7.47	0.98	7.46	26.98	8.02	2.73
MnO	0.46	0.03	0.16	0.00	0.21	0.14	0.16	0.00
MgO	6.49	6.91	5.93	3.02	3.27	4.41	6.37	2.61
CaO	10.39	20.20	10.67	6.40	10.87	29.55	10.75	7.68
Na_2O	0.99	0.07	0.75	0.08	0.52	0.01	0.59	0.03
K_2O	0.54	0.05	0.08	0.00	0.42	0.00	0.12	0.00
P_2O_5	1.60	1.77	0.92	0.87	0.95	2.87	1.31	2.21
Totals	76.25	5.11	64.19	21.25	60.79	150.92	66.32	73.16
	716.23 VRS (trach)		747.09 VRS (trach)					
Sample	avg. (n = 15)	Variance	avg. (n = 15)	Variance				
SiO_2	65.86	2.40	67.24	9.53				
TiO_2	0.20	0.24	0.30	0.49				
Al_2O_3	14.16	2.08	14.04	1.24				
FeO	0.20	0.02	0.41	1.17				
MnO	0.03	0.00	0.02	0.00				
MgO	0.04	0.00	0.14	0.20				
CaO	2.94	0.41	4.02	2.55				
Na_2O	4.01	0.68	3.02	0.37				
K_2O	1.05	1.76	1.00	0.06				
P_2O_5	0.00	0.00	0.06	0.04				
Totals	88.48	8.29	90.26	1.35				

Note: avg.—average; Al—ash lenses; Hyalo—hyaloclastite; LT—lapilli tuff; T—tuff; VD—volcanic diamictite; VRS—volcanic clast-rich sandstone; bas—basanite; palag—palagonite; trach—trachyte. Variance is calculated according the algorithm $n\Sigma x^2 - (\Sigma x^2)/n^2$, where n is the number of the performed analyses and x is the obtained value; variance is a measure of the chemical heterogeneity of different samples (Stroncik and Schmincke, 2001).

and Al/(Al + Si) ratios, but wide ranges in the Mg/(Mg + Fe) ratios.

Three main types of clay minerals, smectite, illite, and chlorite, were observed in the LSU5 sequence. The most abundant clay mineral in the LSU5 is smectite, the content of which ranges between 24% and 100%; the mean value is 91% (Fig. 6). The highest smectite contents (100%) are observed in lapilli tuff and tuff samples.

The smectite in the shallower LSU5 analyzed sample, at 591.85 mbsf, has the highest Mg content (Fig. 7). At depths >591.85 mbsf, smectites found in volcanic clasts and vesicles within hyaloclastites, tuffs and lapilli tuffs, volcaniclastic diamictites, and volcanic-rich mudstones to sandstones have compositions differing only for the Mg/(Mg + Fe) ratio, and all are saponite (Fig. 7). In contrast, the finer grained smectites constituting the intergranular matrix of volcanic clast–rich mudstones to sandstones are richer in Al and trend toward the high-Al smectites defined by the montmorillonite-beidellite field in Figure 7. The illite content in the LSU5 ranges between 0% and 54% (mean value 7%). The amounts of smectite and illite are inversely correlated ($R^2 = -0.98$). The chlorite content ranges from 0% to 22% (mean value 3%; Fig. 6). The ash lens sample with unaltered glass from 575.65 mbsf has the highest illite and chlorite contents, 55% and 22%, respectively. Relatively high illite and chlorite contents can also be found in samples of volcanic clast–rich mudstones to sandstones within LSU5B, between 608.75 and 620.38 mbsf, and in LSU5A at 715.05, 745.12, and 748.97 mbsf. Figure 6 shows the downcore variation in clay minerals abundance.

DISCUSSION

Alteration Zones

The presence of fresh volcanic glass, mineral assemblages, and alteration textures are used to identify three main alteration zones within

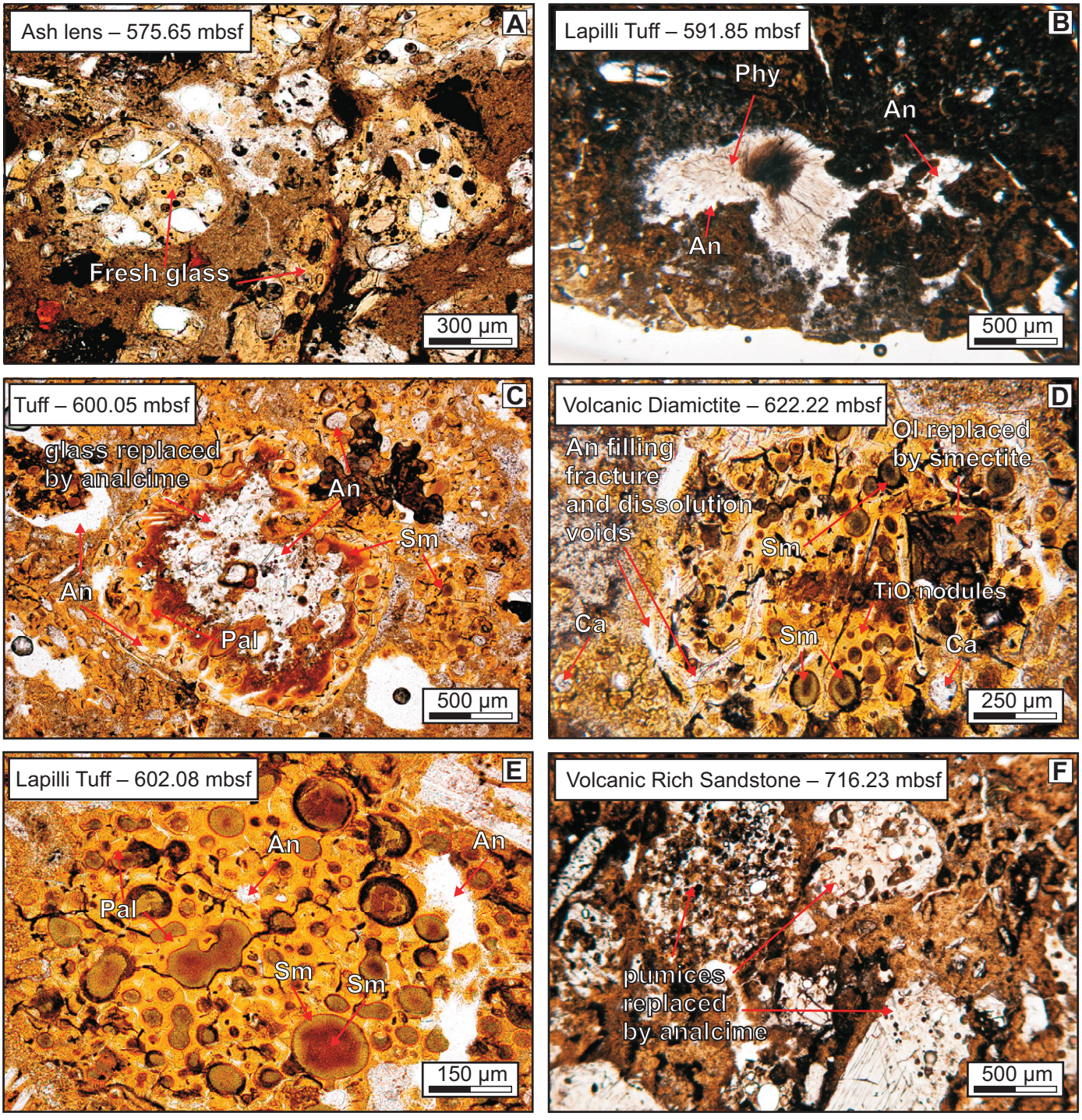

Figure 2. Optical microscope images (plane-polarized light) of representative alteration textures in the analyzed samples. (A) Fresh, vesicular volcanic glass fragments in ash lenses at 575.65 m below seafloor (mbsf) containing abundant plagioclase microlites immersed in a fine-grained matrix of clay minerals (smectite + illite + chlorite). (B) Analcime (An) and phillipsite filling secondary pores in lapilli tuff at 591.85 mbsf; the first zeolite to form is fibrous phillipsite (Phy), followed by analcime. (C) Glass shards within a primary tuff at 600.05 mbsf completely transformed into palagonite (orange glass) and smectite (Sm, dark brown areas) to the point that the original vesicles and grain morphologies are almost obliterated. Grains are cemented by analcime. (D) Volcanic diamictite at 622.22 mbsf; grain fracturing occurred along the outer surface together with minor glass dissolution (presence of TiO_2 micronodules); brown to pale green pore-lining smectite formed in volcanic vesicles and replaced olivine (Ol) crystals. Volcanic glass is completely transformed into palagonite and smectite. Calcite (Ca) and analcime fills vesicles and secondary pores. (E) Tachylitic glass in lapilli tuff at 602.80 mbsf completely transformed into palagonite (Pal); vesicles are filled by analcime. (F) Volcanic glass within volcanic-rich sandstone at 716.23 mbsf; fragments are completely replaced by analcime; predissolution textures such as palagonite and smectite vesicle linings or microlites are preserved.

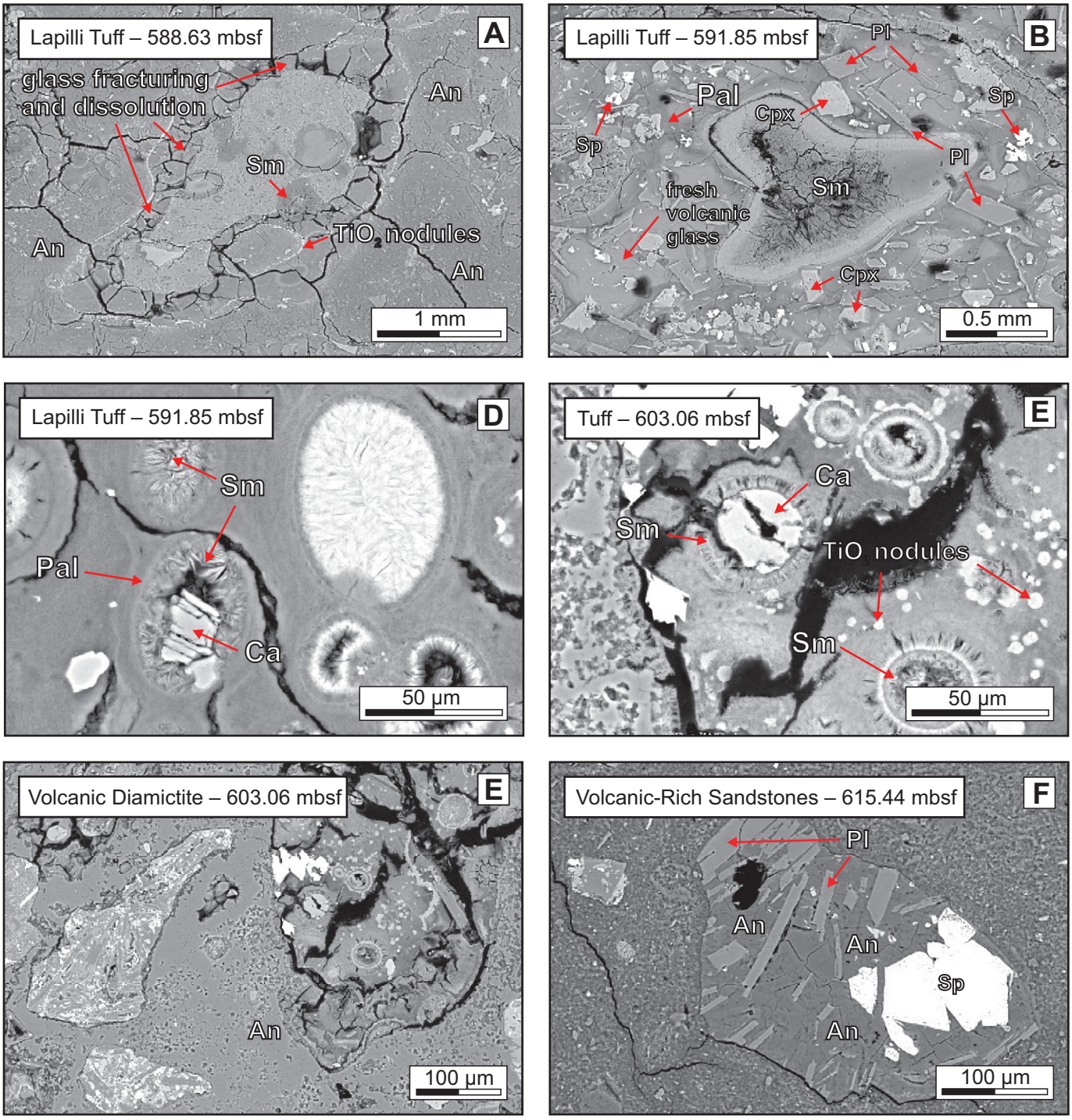

Figure 3. Scanning electron microscope backscattered electron images representative of the main alteration textures and mineral assemblages identified in LSU5 (mbsf—meters below seafloor). (A) Highly fractured outer rim of a vesicular glass shard altered to palagonite; note the alignments of TiO_2 micronodules on the outer and inner surfaces. Vesicles are filled by smectite (Sm). Shards are cemented by analcime (An). (B) Plagioclase (Pl), clinopyroxenes (Cpx), and spinels (Sp) embedded in a glassy matrix with variable degrees of alteration. The darker area is unaltered glass; the brighter area is palagonitized glass (Pal). The large vesicle consists of saponite (Sm). (C) Vesicles in the altered glass consisting of smectitic flakes (Sm), palagonite, and occasionally calcite (Ca) in the core. TiO_2 micronodules are also present. (D) Vesicles have an outer amorphous rim of palagonite (Pal), an inner portion containing smectitic flakes (Sm, saponite) and often calcite in the core. Apatite (Ap) may also grow in the external portion of vesicles. (E) Image of a diamictite consisting of altered volcanic glass and crystal-rich lava fragments. The matrix is composed of analcime. (F) A basaltic clast embedded in a fine detrital matrix consisting of pyroxene, plagioclase, volcanic clasts of various sizes, glass shards (now zeolitized), and fine-grained clay minerals. The large clast in the center consists of spinel (bright white), plagioclase (light gray) and analcime (darker gray).

Geosphere, published online on 6 March 2013 as doi:10.1130/GES00812.1

the studied volcanic sequence. With increasing depth they are: (1) nonaltered (~575–584 mbsf), (2) incipiently to mostly altered (~584–591 mbsf), and (3) fully altered (>591 mbsf). The main textural and mineralogical features of the three alteration zones are summarized in Table 3.

Relationship Between Alteration Zoning and Volcanic Processes

Several factors influence the alteration of volcanic glass, including its chemical composition, the nature of source materials (i.e., glass versus crystalline), the presence of circulating fluids and their composition, pH, pressure, temperature, and/or the porosity of sediments (Stroncik and Schmincke, 2002; Gifkins et al., 2005). Diagenetic alteration of volcanic sequences commonly reflects progressive variation in mineral assemblage due to changes in pore water chemistry, temperature, and pressure with depth of burial (Gifkins et al., 2005), and tends to produce smooth transitions instead of sharp boundaries in alteration intensity. In contrast, the lithology may change abruptly due to rapid variations in the depositional environment or, in a volcanic area, to rapid changes in the eruptive style. Primary and secondary porosities are related to lithology and therefore the variation of these parameters may also be abrupt.

We conclude that the sharp change in alteration intensity observed at ~591 mbsf is unlikely to be the result of gradual changes in physical parameters during burial and diagenesis of glass-rich volcanic sediments, but is more likely a consequence of the style of eruption and environment of deposition and the resulting texture of the primary volcanic deposits. In addition, according to downhole measurements of heat flow and considering the hydrologic characteristics of the AND-1B core (Morin et al., 2010), there is no evidence of a significant postdepositional circulation of hydrothermal fluids that could have produced local variations in the mineral alteration assemblage, microtextures, and chemical compositions.

It was suggested (in Di Roberto et al., 2010) that LSU5B was emplaced during the growth of a volcanic edifice or complex erupting in a transitional environment under submarine to very shallow and/or emergent conditions. The presence of a series of hiatuses between 615.50 and 635.00 mbsf, thought to account for ~1 m.y., and geochronologic data suggest that the LSU5B sequence was deposited over a time span of ~1 m.y. (Wilson et al., 2012); nevertheless, facies architecture suggests that it is more likely that LSU5B was deposited very rapidly by intense submarine volcanic activity accompanied by short periods of quiescence. Recent analogs,

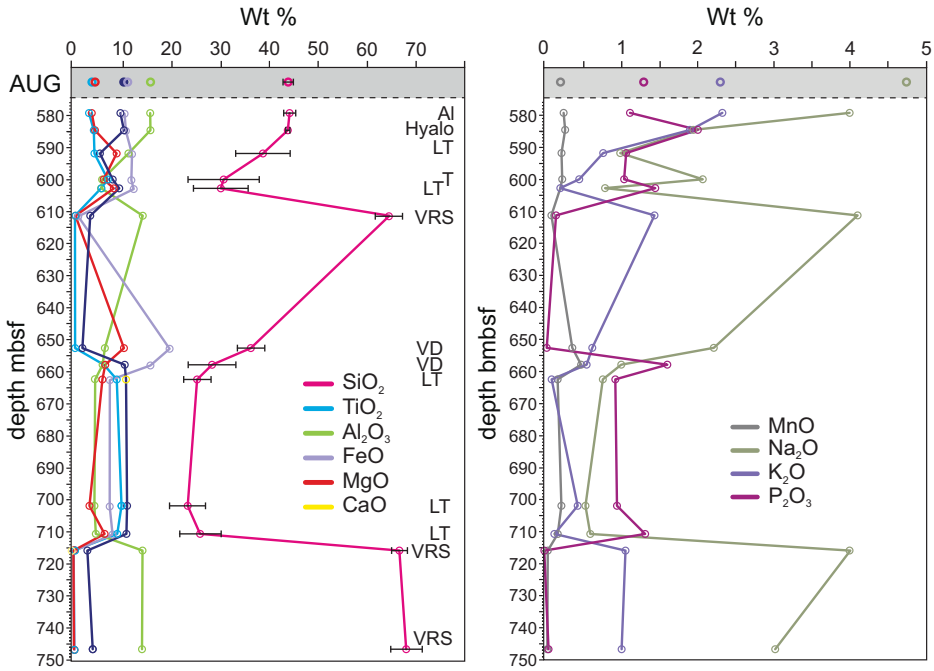

Figure 4. Downcore variations in the composition of volcanic glass or palagonite within studied samples (mbsf—meters below seafloor). All points on this graph are average compositions of all glass or palagonite measured at each depth (data from Table 2). For SiO_2 the ±1σ standard deviation bar is reported to highlight the variability of palagonite composition within each single sample. The average composition of unaltered glass (AUG) is highlighted in gray. Al—ash lenses; Hyalo—hyaloclastite; LT—lapilli tuff; T—tuff; VD—volcanic diamictite; VRS—volcanic clast–rich sandstone.

such as Surtsey (Iceland), Capelinhos (Faial Island, Azores, Portugal), and the ongoing eruption of El Hierro (Canary Islands, Spain), demonstrate that submarine eruptions can construct edifices of as much as several hundred meters in a very short time (a few weeks to less than a few years; Thorarinsson et al., 1964; Machado et al., 1962; Meletlidis et al., 2012) and produce structures similar to those observed in LSU5B.

Assuming that the LSU5B deposits were emplaced over a short time period and that they were altered under generally homogeneous physical and chemical conditions (pH, temperature, composition of circulating fluids), the observed variations in the style of alteration is likely associated to a change in volcanism. Glass fragments above and below ~591 mbsf were emitted in different environments and possibly cooled under different thermal regimes. Glass-bearing pyroclasts in sediments at depths >~591 mbsf may have been emitted at high temperature directly in a water-rich environment, during the submarine stage of an eruption. In contrast, pyroclasts in sediments <~591 mbsf may represent the final shallow-water to emergent stage of an eruption (Di Roberto et al., 2010). At high temperatures volcanic glass alters readily in the presence of abundant alkaline fluids (seawater), whereas the rate of alteration decreases significantly under dry conditions (Gifkins et al., 2005, and references therein). Our hypothesis is confirmed by the results of ongoing studies on sediments from the second AND-2A core site (Southern McMurdo Sound Project), where, for similar thermal borehole properties (Schröder et al., 2011), a large proportion of the basanitic glass considered to have been emitted in a subaerial environment is completely fresh (Di Roberto et al., 2012; Nyland, 2011; Nyland et al., 2012), even in the presence of alkaline fluids (Panter et al., 2008).

The composition of palagonite below ~591 mbsf is almost homogeneous (Table 2; Fig. 4) and does not follow a regular pattern with increasing depth as it would be expected for a burial process; this feature testifies to the absence of significant diagenetic alteration. Small variations in the composition of palagonite, such as those observed in volcanic diamictite at 652.82 mbsf (Table 2; Fig. 4), are comparable with the variability observed within single samples (see 1σ standard deviation; Fig. 4). These variations can be likely related to primary volcanic textures of the deposit, resulting from different emplace-

Geosphere, published online on 6 March 2013 as doi:10.1130/GES00812.1

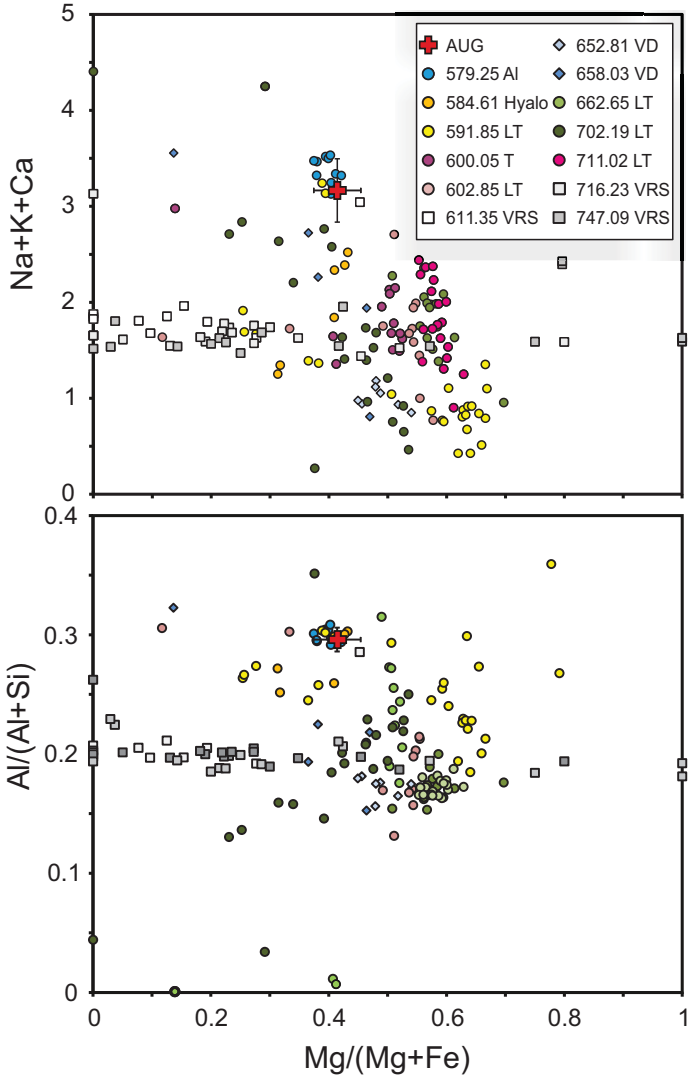

Figure 5. Compositions of pore-lining and glass-replacing palagonite in the Na + Ca + K versus Al/(Al + Si) and in Mg/(Mg + Fe) versus Al/(Al + Si) diagrams (cations were calculated on the basis of 22 oxygen equivalents). Red cross—average unaltered glass (AUG; error at 1σ); circles—composition of altered volcanic glass within ash lenses (Al), tuff (T), lapilli tuff (LT), and hyaloclastite (Hyalo); diamonds—composition of altered volcanic glass within volcanic diamictites (VD); squares—composition of altered volcanic glass within volcanic-rich sandstone (VRS). Numbers in key represent the depth of samples in meters below seafloor (mbsf).

ment dynamics and consequent changing of the physical condition during the reactions with formational fluids (e.g., reduced porosity and/or permeability).

Relationship Between Alteration and Source Material

There appears to be a close relationship between the alteration style and mineral assemblage and the composition of the volcanic glass forming pyroclastic deposits, volcanogenic sedimentary deposits, and resedimented syneruptive volcaniclastic deposits. Geochemical data indicate that vitric fragments forming volcanogenic sandstones contain glass that is more silica-rich and have trachytic to rhyolitic compositions. This would explain the different style of alteration with respect to basanitic glasses forming hyaloclastite, tuff, and volcanic diamictites. It is well known that the primary composition of volcanic glass can influence the alteration style and mineralogy, and that silica-rich glass usually alters less rapidly than more mafic glasses (Hawkins, 1981; Whetten and Hawkins, 1970; Fisher and Schmincke, 1984; Friedman and Long, 1984; Petit et al., 1990; Wolff-Boenisch et al., 2004).

Pyroclastic deposits and extensive volcanic outcrops from the Erebus Volcanic Province likely were present near the drill site at the time of LSU5 deposition (Fig. 1); these included alkali volcanic deposits originating from White Island, Black Island, and Minna Bluff, and the more silica-saturated to silica-oversaturated trachytic-alkaline products from the Mount Morning volcanic complex (Kyle, 1990a, 1990b; Cooper et al., 2007; Martin et al., 2010). It is reasonable that trachytic to rhyolitic glasses were eroded from these on-land pyroclastic deposits and then transported and deposited by fluvial, marine, or glacial processes. The silica-rich glass was fresh and subsequently altered during burial or during subaerial exposure to weathering agents. The detrital nature of trachytic to rhyolitic glass fragments seems to be confirmed by the high degree of mixing between these fragments and nonvolcanic clasts and basement rocks and by the evidence of intense reworking of volcanic clasts within volcanogenic sedimentary deposits (Krissek et al., 2007; Di Roberto et al., 2010). The abundant detrital component of volcanic clast–rich sandstone rocks is also evidenced by the high illite and chlorite content of the clay fraction. Illite, chlorite, and montmorillonitic smectite derived from the physical alteration of basement rocks in the Transantarctic Mountains (Ehrmann et al., 1992). The smectite chemical characteristics proved that newly formed smectites altering volcanic phases inherited the composition of the parent material, mainly the Mg/(Mg + Fe) ratio, whereas detrital smectites deposited together with fine-grained sediments in volcanic clast–rich sandstone have higher Al content because they are derived from the physical degradation of source rocks on land (Ehrmann et al., 2005; Giorgetti et al., 2007). Variations of smectite composition and clay mineral assemblage in the alteration zones are not correlated with depth, but they do depend on lithologies and primary glass nature.

CONCLUSIONS

A detailed investigation of alteration texture, mineralogy, and geochemistry in the AND-1B core volcanic succession revealed the presence of three separate zones characterized by different degrees of alteration: (1) nonaltered, (2) incipiently to mostly altered, and (3) fully altered.

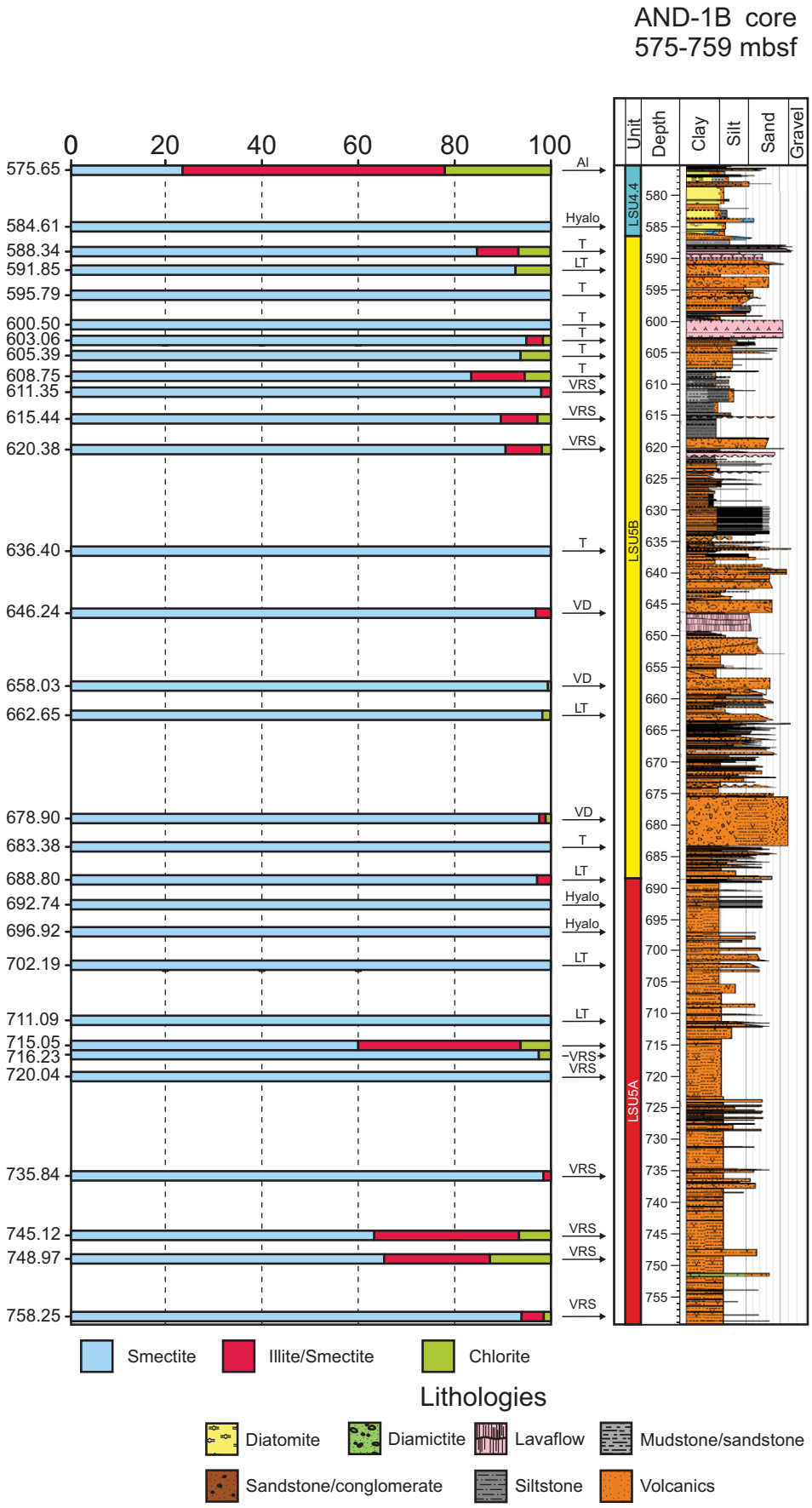

Figure 6. Downcore variations in clay mineral contents within studied samples (mbsf—meters below seafloor). The abundance of main clay minerals (smectite, illite, chlorite, and kaolinite) was estimated using the weighting factors of Biscaye (1965) on diffractograms. Clay mineral percentage standard deviations were calculated using the results of 10 diffractograms obtained from 10 oriented mounts prepared from a single sample. Standard deviations were illite ±1%, smectite ±1%, chlorite ±2.5%, and kaolinite ±2%. Samples are reported in the summary stratigraphic column of the LSU 4.4, LSU5A, and LSU5B. LT—lapilli tuff; T—tuff; VRS—volcanic clast–rich sandstone; VD—volcanic diamictite.

TABLE 3. ALTERATION ZONES

Depth (mbsf)	Environment of origin and deposition mechanism	Alteration	Alteration minerals	Alteration textures	Glass
574–584	Mainly subaerial by pyroclastic surge and/or fallout	None to marginal	None	None	Fresh
584–591	Subaerial to shallow-water by pyroclastic fallout and/or subaqueous fall and eruption-fed density currents	Incipient to pervasive	Palagonite + Ti oxides + smectite + phillipsite ± analcime ± calcite	Grain fracturing, glass dissolution, partial glass conversion into palagonite. Palagonite ± smectite pore linings. Phillipsite ± calcite ± analcime pore filling. Vitric fragment original shape is mostly preserved.	Sparse fresh
>591	Submarine for subaqueous fall and/or eruption-fed density currents (T and LT) or water-supported, cohesionless debris flows (VD)	Complete	Palagonite + Ti oxides + smectite + analcime + calcite + apatite	Grain fracturing. Pervasive glass dissolution and complete conversion into palagonite. Analcime + calcite + clay minerals fill porosity created by glass dissolution (to complete grain replacement). Smectite grain coating, smectite + palagonite pore lining. Vitric fragment original shape is modified to completely destroyed.	Completely altered

Note: mbsf—meters below seafloor; T—tuff; LT—lapilli tuff; VD—volcanic diamictite.

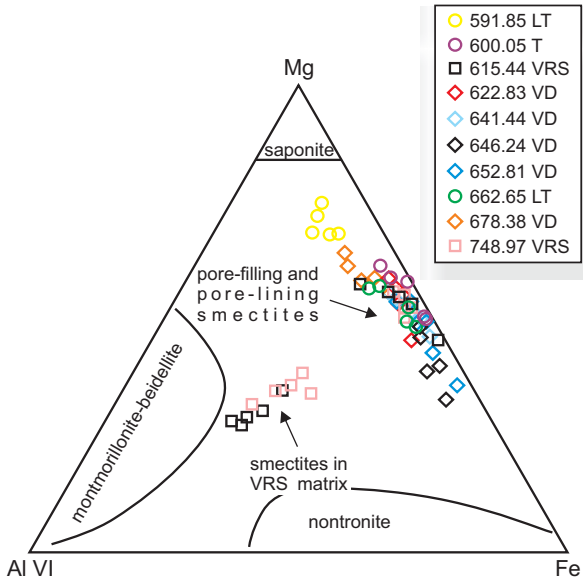

Figure 7. Triangular diagram showing the Al(VI)-Mg-Fe cation distribution in smectites from representative samples. Note that pore-filling and pore-lining smectites formed by alteration of volcanic glass within all types of sediments are all saponite (trioctahedral smectite) with variable Fe/Mg ratios, whereas smectites in the fine-grained matrix of volcanic clast–rich sandstones trend toward montmorillonite-beidellite (dioctahedral smectites) field. Al—ash lenses; Hyalo—hyaloclastite; LT—lapilli tuff; T—tuff; VD—volcanic diamictite; VRS—volcanic clast–rich sandstone. Numbers in key represent the depth of samples in meters below seafloor (mbsf).

The lack of intense alteration of volcanic glass at depths shallower than 591 mbsf is in agreement with the results presented in Di Roberto et al. (2010), according to which this part of the sequence was formed by the explosive activity of a subaerial volcano under mostly dry, open atmosphere conditions. The sharp transition between incipiently to mostly altered rocks and fully altered rocks (~591 mbsf) cannot be fully explained by postdepositional diagenetic processes. It is likely due to the texture of the primary volcanic deposits and to paleodepositional conditions, which are related to the eruptive style and the degree of fragmentation of the erupted material. In contrast, the alteration zoning of volcanic detritus in the underlying zone (>591 mbsf) is coherent with a stage of subaqueous growth of the volcanic edifice, during which volcanic glass–rich materials interacted with fluids (seawater or fresh water) at high temperatures. This general alteration trend is further complicated by the more silica-rich composition of volcanic glass derived from the reworking of pyroclasts from earlier volcanic activity.

ACKNOWLEDGMENTS

The ANDRILL (Antarctic Geological Drilling) project is a multinational collaboration between the Antarctic programs of Germany, Italy, New Zealand, and the United States. Antarctica New Zealand is the project operator and developed the drilling system in collaboration with A. Pyne. Antarctica New Zealand supported the drilling team at Scott Base; Raytheon Polar Services Corporation supported the science team at McMurdo Station and the Crary Science and Engineering Laboratory. The ANDRILL Science Management Office at the University of Nebraska-Lincoln provided science planning and operational support. The scientific studies are jointly supported by the U.S. National Science Foundation, the New Zealand Foundation for Research Science and Technology, the Italian Antarctic Research Programme, the German Research Foundation, and the Alfred Wegener Institute for Polar and Marine Research. We are grateful for the detailed core logging by the McMurdo Ice Shelf Sedimentology Team and for helpful discussions with Phil Kyle during the drilling. We thank cochiefs Tim Naish and Ross Powell and staff scientist Richard Levy for coordinating efforts, and A. Cavallo (Istituto Nazionale di Geofisica e Vulcanologia, Rome) for assistance with electron microprobe analyses. Di Roberto benefited from a Programme for Antarctic Research postdoctoral fellowship. K.S. Panter and an anonymous reviewer are also acknowledged for their accurate and critical comments that greatly improved the manuscript.

REFERENCES CITED

Armstrong, R.L., 1978, K-Ar dating: Late Cenozoic McMurdo Volcanic Group and Dry Valley glacial history, Victoria Land, Antarctica: New Zealand Journal of Geology and Geophysics, v. 21, p. 685–698, doi:10.1080/00288306.1978.10425199.

Biscaye, P.E., 1965, Mineralogy and sedimentation of recent deep-sea clays in the Atlantic Ocean and adjacent seas and oceans: Geological Society of America Bulletin, v. 76, p. 803–832, doi:10.1130/0016-7606(1965)76[803:MASORD]2.0.CO;2.

Cooper, A., Adam, L., Coulter, R., Eby, G., and McIntosh, W., 2007, Geology, geochronology and geochemistry of a basanitic volcano, White Island, Ross Sea, Antarctica: Journal of Volcanology and Geothermal Research, v. 165, p. 189–216, doi:10.1016/j.jvolgeores.2007.06.003.

Del Carlo, P., Panter, K.S., Bassett, K., Bracciali, L., Di Vincenzo, G., and Rocchi, S., 2009, The upper lithostratigraphic unit of ANDRILL AND-2A core (Southern McMurdo Sound, Antarctica): Local volcanic sources, paleoenvironmental implications and subsidence in the western Victoria Land Basin: Global and Planetary Change, v. 69, p. 142–161, doi:10.1016/j.gloplacha.2009.09.002.

Di Roberto, A., Pompilio, M., and Wilch, T.I., 2010, Late Miocene submarine volcanism in ANDRILL AND-1B drill core, Ross Embayment, Antarctica: Geosphere, v. 6, p. 524–536, doi:10.1130/GES00537.1.

Di Roberto, A., Del Carlo, P., Rocchi, S., and Panter, K.S., 2012, Early Miocene volcanic activity and paleoenvironment conditions recorded in tephra layers of the AND-2A core (southern McMurdo Sound, Antarctica): Geosphere, v. 8, p. 1342–1355, doi:10.1130/GES00754.1.

Ehrmann, W.U., Melles, M., Kuhn, G., and Grobe, H., 1992, Significance of clay mineral assemblage in the Antarctic Ocean: Marine Geology, v. 107, p. 249–273, doi:10.1016/0025-3227(92)90075-S.

Ehrmann, W., Setti, M., and Marinoni, L., 2005, Clay minerals in Cenozoic sediments off Cape Roberts (McMurdo Sound, Antarctica) reveal palaeoclimatic history: Palaeogeography, Palaeoclimatology, Palaeoecology, v. 229, p. 187–211, doi:10.1016/j.palaeo.2005.06.022.

Esser, R.P., Kyle, P.R., and McIntosh, W.C., 2004, $^{40}Ar/^{39}Ar$ dating of the eruptive history of Mt. Erebus, Antarctica: Volcano evolution: Bulletin of Volcanology, v. 66, p. 671–686, doi:10.1007/s00445-004-0354-x.

Fisher, R.V., and Schmincke, H.-U., 1984, Pyroclastic rocks: New York, Springer-Verlag, 472 p.

Friedman, I., and Long, W., 1984, Volcanic glasses—Their origins and alteration processes: Journal of Non-Crystalline Solids, v. 67, p. 127–133, doi:10.1016/0022-3093(84)90144-3.

Gifkins, C.C., Herrmann, W., and Large, R.R., 2005, Altered volcanic rocks: A guide to description and interpretation: University of Tasmania Centre for Ore Deposit Research, 275 p.

Giorgetti, G., Aghib, F.S., Livi, K.J.T., Gaillot, A.C., and Wilson, T.J., 2007, Newly formed phyllosilicates in rock matrices and fractures from CRP-3 core (Antarctica): An electron microscopy study: Clay Minerals, v. 42, p. 21–43, doi:10.1180/claymin.2007.042.1.03.

Hawkins, D.B., 1981, Kinetics of glass dissolution and zeolite formation under hydrothermal conditions: Clays and Clay Minerals, v. 29, p. 331–340, doi:10.1346/CCMN.1981.0290503.

Honnorez, J., 1981, The aging of the oceanic lithosphere, *in* Emiliani C., ed., The oceanic lithosphere: New York, John Wiley, p. 525–587.

Houghton, B.F., and Wilson, C.J.N., 1989, A vesicularity index for pyroclastic deposits: Bulletin of Volcanology, v. 51, p. 451–462, doi:10.1007/BF01078811.

Krissek, L., Browne, G., Carter, L., Cowan, E., Dunbar, G., McKay, R., Naish, T., Powell, R., Reed, J., Wilch, T., and The Andrill-MIS Science Team, 2007, Sedimentology and stratigraphy of the AND-1B Core, ANDRILL McMurdo Ice Shelf Project, Antarctica: Terra Antartica, v. 14, p. 185–222.

Kyle, P.R., 1981, Mineralogy and geochemistry of a basanite to phonolite sequence at Hut Point Peninsula, Antarctica, based on core from Dry Valley Drilling Project Drillholes 1, 2 and 3: Journal of Petrology, v. 22, p. 451–500, doi:10.1093/petrology/22.4.451.

Kyle, P.R., 1990a, McMurdo Volcanic Group Western Ross Embayment—Introduction, *in* LeMasurier, W.E., and Thomson, J.W., eds., Volcanoes of the Antarctic plate and southern oceans: American Geophysical Union Antarctic Research Series, v. 48, p. 19–25.

Kyle, P.R., 1990b, McMurdo Volcanic Group Western Ross Embayment—Erebus Volcanic Province—Summary, *in* LeMasurier, W.E., and Thomson, J.W., eds., Volcanoes of the Antarctic plate and southern oceans: American Geophysical Union Antarctic Research Series, v. 48, p. 81–88.

Kyle, P.R., and Cole, J.W., 1974, Structural control of volcanism in the McMurdo Volcanic Group, Antarctica: Bulletin of Volcanology, v. 38, p. 16–25, doi:10.1007/BF02597798.

Kyle, P.R., and Muncy, H.L., 1989, Geology and geochronology of McMurdo Volcanic Group rocks in the vicinity of Lake Morning, McMurdo Sound, Antarctica: Antarctic Science, v. 1, p. 345–350, doi:10.1017/S0954102089000520.

Lewis, A.R., Marchant, D.R., Ashworth, A.C., Hemming, S.R., and Machlus, M.L., 2007, Major middle Miocene global climate change: Evidence from East Antarctica and the Transantarctic Mountains: Geological Society of America Bulletin, v. 119, p. 1449–1461, doi:10.1130B26134.1.

Machado, F., Parsons, W.H., Richards, A.F., and Mulford, J.W., 1962, Capelinhos eruption of Fayal volcano, Azores, 1957–1958: Journal of Geophysical Research, v. 67, p. 3519–3529, doi:10.1029/JZ067i009p03519.

Marchant, D.R., Denton, G.H., Swisher, C.C., III, and Potter, N., Jr., 1996, Late Cenozoic Antarctic paleoclimate reconstructed from volcanic ashes in the Dry Valleys region of southern Victoria Land: Geological Society of America Bulletin, v. 108, p. 181–194, doi:10.1130/0016-7606(1996)108<0181:LCAPRF>2.3.CO;2.

Martin, A., Cooper, A., and Dunlap, W., 2010, Geochronology of Mt. Morning, Antarctica: Two-phase evolution of a long-lived trachyte-basanite-phonolite eruptive center: Bulletin of Volcanology, v. 72, p. 357–371, doi:10.1007/s00445-009-0319-1.

Mayewski, P.A., 1975, Glacial geology and late Cenozoic history of the Transantarctic Mountains, Antarctica: Columbus, Ohio State University Institute of Polar Studies Report 56, 168 p.

McKay, R., Browne, G., Carter, L., Cowan, E., Dunbar, G., Krissek, L., Naish, T., Powell, R., Reed, J., Talarico, F., and Wilch, T., 2009, The stratigraphic signature of the late Cenozoic Antarctic Ice Sheets in the Ross Embayment: Geological Society of America Bulletin, v. 121, p. 1537–1561, doi:10.1130/B26540.1.

McKelvey, B.C., Webb, P.N., Harwood, D.M., and Mabin, M.C.G., 1991, The Dominion Range Sirius Group: A record of the late Pliocene–early Pleistocene Beardmore Glacier, *in* Thomson, M.R.A., et al., eds., Geological evolution of Antarctica: Cambridge, UK, Cambridge University Press, p. 675–682.

McPhie, J., Doyle, M., and Allen, R.L., 1993, Volcanic textures: A guide to the interpretation of textures in volcanic rocks: University of Tasmania Centre for Ore Deposit and Exploration Studies, 198 p.

Mercer, J.H., 1968, Glacial geology of the Reedy glacier area, Antarctica: Geological Society of America Bulletin, v. 79, p. 471–486, doi:10.1130/0016-7606(1968)79[471:GGOTRG]2.0.CO;2.

Meletlidis, S., Di Roberto, A., Pompilio, M., Bertagnini, A., Iribarren, I., Felpeto, A., Torres, P.A., and D'Oriano, C., 2012, Xenopumices from the 2011–2012 submarine eruption of El Hierro (Canary Islands, Spain): Constraints on the plumbing system and magma ascent: Geophysical Research Letters, v. 39, doi:10.1029/2012GL052675.

Morin, R.H., Williams, T., Henrys, S.A., Magens, D., Niessen, F., and Hansaraj, D., 2010, Heat flow and hydrologic characteristics at the AND-1B borehole, ANDRILL McMurdo Ice Shelf Project, Antarctica: Geosphere, v. 6, p. 370–378, doi:10.1130/GES00512.1.

Naish, T.R., Powell, R.D., Levy, R., Henrys, S., Krissek, L., Niessen, F., Pompilio, M., Scherer, R., and Wilson, G., 2007, Synthesis of the initial scientific results of the MIS Project (AND-1B Core), Victoria Land Basin, Antarctica: Terra Antartica, v. 14, p. 317–327.

Naish, T., and 55 others, 2009, Obliquity-paced Pliocene West Antarctic ice sheet oscillations: Nature, v. 458, p. 322–328, doi:10.1038/nature07867.

Nyland, R., 2011, Evidence for early-phase explosive basaltic volcanism at Mt. Morning from glass-rich sediments in the ANDRILL AND-2A core and possible response to glacial cyclicity [M.S. thesis]: Bowling Green, Ohio, Bowling Green State University, 158 p.

Nyland, R.E., Panter, K.S., Rocchi, S., Di Vincenzo, G., Del Carlo, P., Tiepolo, M., Field, B., and Gorsevski, P., 2012, Volcanic activity and its link to glaciation cycles: Single-grain age and geochemistry of Early Miocene volcanic glass from ANDRILL AND-2A core, Antarctica: Journal of Volcanology and Geothermal Research, v. 250, p. 106–128, doi:10.1016/j.jvolgeores.2012.11.008.

Panter, K.S., and 14 others, 2008, Petrologic and geochemical composition of the AND-2A core, ANDRILL Southern McMurdo Sound Project, Antarctica, *in* Harwood, D.M., et al., eds., Studies from the ANDRILL, Southern McMurdo Sound Project, Antarctica: Terra Antarctica, v. 15, p. 147–192.

Petit, J.-C., della Mea, G., Dran, J.C., Magonthier, M.C., Mando, P.A., and Paccagnella, A., 1990, Hydrated-layer formation during dissolution of complex silicate glasses and minerals: Geochimica et Cosmochimica Acta, v. 54, p. 1941–1955, doi:10.1016/0016-7037(90)90263-K.

Petschick, R., 2001, MacDiff 4.2.5: http://www.geol-pal.uni-frankfurt.de/Staff/Homepages/Petschick/MacDiff/MacDiffInfoE.html.

Petschick, R., Kuhn, G., and Gingele, F., 1996, Clay mineral distribution in surface sediments of the South Atlantic: Sources, transport, and relation to oceanography: Marine Geology, v. 130, p. 203–229, doi:10.1016/0025-3227(95)00148-4.

Pompilio, M., Dunbar, N., Gebhardt, A.C., Helling, D., Kuhn, G., Kyle, P., McKay, R., Talarico, F., Tulaczyk, S., Vogel, S., and Wilch, T., and the ANDRILL-MIS Science Team, 2007, Petrology and geochemistry of the AND-1B Core, ANDRILL McMurdo Ice Shelf Project, Antarctica: Terra Antartica, v. 14, p. 255–288.

Schiffman, P., Spero, H.J., Southard, R.J., and Swanson, D.A., 2000, Controls on palagonitization versus pedogenic weathering of basaltic tephra: Evidence from the consolidation and geochemistry of the Keanakako'I Ash Member, Kilauea Volcano: Geochemistry Geophysics Geosystems, v. 1, 1040, doi:10.1029/2000GC000068.

Schröder, H., Paulsen, T., and Wonik, T., 2011, Thermal properties of the AND-2A borehole in the southern Victoria Land Basin, McMurdo Sound, Antarctica: Geosphere, v. 7, p. 1324–1330, doi:10.1130/GES00690.1.

Singer, A., and Banin, A., 1990, Characteristics and mode of formation of palagonite: A review: Proceedings of the 9th International Clay Conference, Strasbourg, p. 173–181.

Stroncik, N.A., and Schmincke, H.-U., 2001, Evolution of palagonite: Crystallization, chemical changes, and element budget: Geochemistry Geophysics Geosystems, v. 2, 1017, doi:10.1029/2000GC000102.

Stroncik, N.A., and Schmincke, H.-U., 2002, Palagonite—A review: International Journal of Earth Sciences, v. 91, p. 680–697, doi:10.1007/s00531-001-0238-7.

Tauxe, L., Gans, P., and Mankinen, E.A., 2004, Paleomagnetism and ^{40}Ar-^{39}Ar ages from volcanics extruded during the Matuyama and Brunhes Chrons near McMurdo Sound, Antarctica: Geochemistry Geophysics Geosystems, v. 5, doi:10.1029/2003GC000656.

Thorarinsson, S., Einarsson, T., Tigvaldason, G.E., and Elisson, G., 1964, The submarine eruption off the Westmann Islands 1963–1964: Bulletin Volcanologique, v. 27, p. 435–445, doi:10.1007/BF02597544.

Timms, C.J., 2006, Reconstruction of a grounded ice sheet in McMurdo Sound—Evidence from southern Black Island, Antarctica [M.S. thesis]: Dunedin, New Zealand, University of Otago, 150 p.

Walton, A.W., and Schiffman, P., 2003, Alteration of hyaloclastite in the HSDP 2 Phase 1 Drill Core 1. Description and paragenesis: Geochemistry Geophysics Geosystems, v. 4, 8709, doi:10.1029/2002GC000368.

Whetten, J.T., and Hawkins, J.W., 1970, Diagenetic origin of greywacke matrix minerals: Sedimentology, v. 15, p. 347–361, doi:10.1111/j.1365-3091.1970.tb02191.x.

White, J.D.L., 2000, Subaqueous eruption-fed density currents and their deposits: Precambrian Research, v. 101, p. 87–109, doi:10.1016/S0301-9268(99)00096-0.

Wilch, T.I., Lux, D.R., Denton, G.H., and McIntosh, W.C., 1993, Minimal Pliocene–Pleistocene uplift of the dry valleys sector of the Transantarctic Mountains: A key parameter in ice-sheet reconstructions: Geology, v. 21, p. 841–844, doi:10.1130/0091-7613(1993)021<0841:MPPUOT>2.3.CO;2.

Wilch, T.I., McIntosh, W.C., Panter, K.S., Dunbar, N.W., Smellie, J.L., Fargo, A., Scanlan, M., Zimmerer, M.J., Ross, J., and Bosket, M.E., 2008, Volcanic and glacial geology of the Miocene Minna Bluff Volcanic Complex, Antarctica: Eos (Transactions, American Geophysical Union), v. 89, fall meeting supplement, abs. V11F–06.

Wilson, G.S., and 63 others, 2012, Neogene tectonic and climatic evolution of the Western Ross Sea, Antarctica—Chronology of events from the AND-1B drill hole: Global and Planetary Change, v. 96–97, p. 189–203, doi:10.1016/j.gloplacha.2012.05.019.

Wolff-Boenisch, D., Gislason, S.R., Oelkers, E.H., and Putnis, C.V., 2004, The dissolution rates of natural glasses as a function of their composition at ph 4 and 10.6, and temperatures from 25 to 74°C: Geochimica et Cosmochimica Acta, v. 68, p. 4843–4858, doi:10.1016/j.gca.2004.05.027.

Wright, A.C., and Kyle, P.R., 1990a, McMurdo Volcanic Group Western Ross Embayment—Individual volcano descriptions—Mount Bird, *in* LeMasurier, W.E., and Thomson, J.W., eds., Volcanoes of the Antarctic plate and southern oceans: American Geophysical Union Antarctic Research Series, v. 48, p. 97–98.

Wright, A.C., and Kyle, P.R., 1990b, McMurdo Volcanic Group Western Ross Embayment—Individual volcano descriptions—Mount Terror, *in* LeMasurier, W.E., and Thomson, J.W., eds., Volcanoes of the Antarctic plate and southern oceans: American Geophysical Union Antarctic Research Series, v. 48, p. 99–102.

Geosphere, published online on 6 March 2013 as doi:10.1130/GES00812.1

Geosphere

Alteration of volcanic deposits in the ANDRILL AND-1B core: Influence of paleodeposition, eruptive style, and magmatic composition

Alessio Di Roberto, Giovanna Giorgetti, Francesco Iacoviello and Massimo Pompilio

Geosphere published online 6 March 2013;
doi: 10.1130/GES00812.1

Email alerting services click www.gsapubs.org/cgi/alerts to receive free e-mail alerts when new articles cite this article

Subscribe click www.gsapubs.org/subscriptions/ to subscribe to Geosphere

Permission request click http://www.geosociety.org/pubs/copyrt.htm#gsa to contact GSA

Copyright not claimed on content prepared wholly by U.S. government employees within scope of their employment. Individual scientists are hereby granted permission, without fees or further requests to GSA, to use a single figure, a single table, and/or a brief paragraph of text in subsequent works and to make unlimited copies of items in GSA's journals for noncommercial use in classrooms to further education and science. This file may not be posted to any Web site, but authors may post the abstracts only of their articles on their own or their organization's Web site providing the posting includes a reference to the article's full citation. GSA provides this and other forums for the presentation of diverse opinions and positions by scientists worldwide, regardless of their race, citizenship, gender, religion, or political viewpoint. Opinions presented in this publication do not reflect official positions of the Society.

Notes

Advance online articles have been peer reviewed and accepted for publication but have not yet appeared in the paper journal (edited, typeset versions may be posted when available prior to final publication). Advance online articles are citable and establish publication priority; they are indexed by GeoRef from initial publication. Citations to Advance online articles must include the digital object identifier (DOIs) and date of initial publication.

© Geological Society of America

THE GEOLOGICAL SOCIETY OF AMERICA